Protein Science (1994), *3*:118–125. Cambridge University Press. Printed in the USA.

Positions of His-64 and a bound water in human carbonic anhydrase II upon binding three structurally related inhibitors

GRAHAM M. SMITH,[1] RICHARD S. ALEXANDER,[2,4] DAVID W. CHRISTIANSON,[2] BRIAN M. McKEEVER,[3] GERALD S. PONTICELLO,[1] JAMES P. SPRINGER,[3] WILLIAM C. RANDALL,[1] JOHN J. BALDWIN,[1,5] AND CHARLES N. HABECKER[1]

[1] Merck Research Laboratories, West Point, Pennsylvania 19486
[2] Department of Chemistry, University of Pennsylvania, Philadelphia, Pennsylvania 19104-6323
[3] Merck Research Laboratories, Rahway, New Jersey 07065

(RECEIVED July 31, 1993; ACCEPTED October 28, 1993)

Abstract

The 3-dimensional structure of human carbonic anhydrase II (HCAII; EC 4.2.1.1) complexed with 3 structurally related inhibitors, *1a*, *1b*, and *1c*, has been determined by X-ray crystallographic methods. The 3 inhibitors (*1a* = $C_8H_{12}N_2O_4S_3$) vary only in the length of the substituent on the 4-amino group: *1a*, proton; *1b*, methyl; and *1c*, ethyl. The binding constants (K_i's) for *1a*, *1b*, and *1c* to HCAII are 1.52, 1.88, and 0.37 nM, respectively. These structures were solved to learn if any structural cause could be found for the difference in binding. In the complex with inhibitors *1a* and *1b*, electron density can be observed for His-64 and a bound water molecule in the native positions. When inhibitor *1c* is bound, the side chain attached to the 4-amino group is positioned so that His-64 can only occupy the alternate position and the bound water is absent. While a variety of factors contribute to the observed binding constants, the major reason *1c* binds tighter to HCAII than does *1a* or *1b* appears to be entropy: the increase in entropy when the bound water molecule is released contributes to the increase in binding and overcomes the small penalty for putting the His-64 side chain in a higher energy state.

Keywords: entropy; solvation; X-ray crystallography

Human carbonic anhydrase II is a single polypeptide chain containing 259 amino acids and 1 essential zinc ion bound by 3 histidine residues (Pocker & Sarkanen, 1978). The primary function of HCAII is to catalyze the physiologically important equilibrium (Maren, 1967)

$$CO_2 + H_2O \leftrightarrow HCO_3^- + H^+.$$

In particular, HCAII has been found to play a pivotal role in the regulation of intraocular pressure; inhibition of this enzyme is thus an efficient method of regulating aqueous humor dynamics (Prugh et al., 1991). To assist in the development of new inhibitors, we have used X-ray crystallography, molecular graphics, and force field methods to evaluate the contacts between the active site residues and the inhibitors in an attempt to understand the factors and forces responsible for the differences in their measured binding constants. Although accurate quantitative prediction of binding constants for inhibitors bound to HCAII remains a major challenge, this work provides an approach to gain important qualitative insights into ligand–macromolecule interactions.

The 3D structure of native HCAII was first reported in 1972 (Liljas et al., 1972) and updated in 1988 (Eriksson et al., 1988). This system has evolved into a useful model for studying inhibitor–enzyme interactions, because there is very little movement in the active site upon binding a variety of compounds that are themselves small molecules with few conformational degrees of freedom. The binding of several inhibitors has been observed to cause the side chain of His-64 to move away from its native position, with the displacement of the adjacent ordered water[6]

Reprint requests to: Graham M. Smith, Department of Medicinal Chemistry, Merck Research Laboratories, WP42-3, West Point, Pennsylvania 19486.

[4] Present address: Sterling Winthrop Pharmaceuticals Research Division, Collegeville, Pennsylvania 19426-0900.

[5] Present address: Pharmacopia, Princeton, New Jersey 08540.

[6] It has been suggested that the electron density next to the native position of His-64 that was originally called a water may be a low-occupancy conformation of the side chain of His-64 (Krebs et al., 1991) or a combination of a low-occupancy conformation and water. While acknowledging this possibility, we believe the density is primarily a water molecule because it is spherical, has a *B*-factor of 13 Å^2, is not connected by density to the protein backbone, and is a hydrogen bonding distance from the native side chain conformation of His-64.

(Baldwin et al., 1989; Prugh et al., 1991; J.P. Springer et al., unpubl. experiments). Movement of the side chain of His-64 has also been implicated in the enzyme mechanism (Tu et al., 1989; Krebs et al., 1991; Nair & Christianson, 1991). Therefore, the observation of a change in the position of the side chain of His-64 between the native enzyme (Eriksson et al., 1988) and that inhibited by *1c* (Baldwin et al., 1992) (Fig. 1) led us to the question of whether inhibitors *1a* and *1b*, with shorter side chains on the nitrogen, would also alter the position of His-64 and the adjacent water. Preliminary modeling studies with *1a* and *1b* were performed to evaluate this point and suggested that, because of the reduced steric volume, the side chain of His-64 could remain in its native position upon complex formation. We also wanted to use this conformational information to understand the origin of the 4–5-fold difference in binding between inhibitors *1a* and *1b* and inhibitor *1c* (see Table 1). The differences in binding listed in Table 1 are significant based on the number of trials done with each and the resulting standard deviation. In addition, the conditions used in the K_i measurements were as similar to those used in the crystallization experiments as possible. The buffer and the pH were the same, although the concentration of protein was higher in the crystallization. The X-ray studies reported in this paper were done to learn if conformational changes in the inhibitors or the protein could explain the observed differences in the measured binding.

Discussion

In a continuing effort to understand the factors responsible for the binding of inhibitors within the active site of proteins, we examined the 3 compounds (*1a–1c*) bound to HCAII (see Kinemage 1). Structurally these differed only by addition of methyl and ethyl groups to the 4-amino group. Despite the similarity, the measured binding (Ponticello et al., 1987) of these inhibitors at pH 7.4 does not smoothly increase with these structural changes (Table 1). The binding constants for *1a* and *1b* are identical within experimental error, whereas *1c* has a binding constant suggesting 4–5 times greater affinity for the enzyme. Reviewing the enzyme/inhibitor structures reveals that they have a very similar conformation and orientation in the active site (Fig. 2; Kinemage 1). The RMS deviation between the common inhibitor atoms ranges from 0.07 to 0.14 Å. The only differences that appear in the active site of the HCAII/*1c* complex are the change in the position of the side chain of His-64 and loss of a potentially ordered water molecule. In the case of the complexes of inhibitors *1a* and *1b*, it was possible for His-64 to remain in the native position with its adjacent hydrogen bonded water molecule. The distances between the Nε of His-64 and the adjacent water in the native, *1a*, and *1b* structures are within hydrogen bonding distance, at 3.11, 2.86, and 2.71 Å, respectively.

Table 1. *Inhibitor binding constants measured at 37 °C, pH 7.4*

Inhibitor	K_i (nM)	SD	Trials
1a (-NH_2)	1.52	0.20	6
1b (-NH-CH_3)	1.88	0.18	6
1c (-NH-CH_2-CH_3)	0.372	0.085	8

To examine this more carefully, omit maps of His-64 were created in which the full residue and the adjacent water were removed from the structure. To reduce the bias in the omit maps, each structure was refined with X-PLOR before the maps were created. The native $|F_o| - |F_c|$ map, contoured at 2σ (Fig. 3D), shows density that clearly indicates that the side chain occupies primarily the native position. The density in the alternative position appears to be indicative of a water molecule. However, it is known that the side chain of His-64 is in a fairly delicate conformational balance. Evidence for this comes from previous work that showed that the location of the side chain switches to the alternate position when Thr-200 is mutated to serine (Krebs et al., 1991), when the pH is changed from 8.0 to 5.7 (Nair & Christianson, 1991), and when the zinc ligand His-94 is mutated to Cys (R.S. Alexander, L. Kiefer, C.A. Fierke, & D.W. Christianson, unpubl. results). It has also been inferred from mutagenesis work (Tu et al., 1989) that His-64 is an integral part of the HCAII enzyme mechanism acting as a "shuttle" for proton transfer, implying side chain movement. Omit maps for *1a* (Fig. 3A) and *1b* (Fig. 3B) are consistent with the His-64 side chain being primarily in the native position.[7] However, the shape of the electron density indicates that in the HCAII/*1b* complex (Fig. 3B) the equilibrium may be starting to shift to the alternative side chain conformation. The situation is quite different in *1c* (Fig. 3C), where the ethyl side chain on the inhibitor appears to force the His-64 side chain completely into the alternate position, eliminating its potential mobility. As a measure of the van der Waals energy that each inhibitor might derive from the increase in length of the 4-amino side chain, a list (Table 2) of all atomic contacts within 4.50 Å was made for each inhibitor. From this list it can be seen that each addition to the side chain causes an increase in the number of contacts,

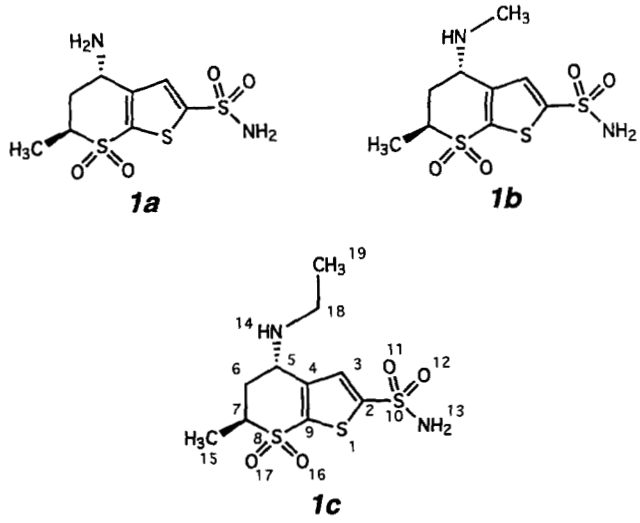

Fig. 1. Inhibitor structures *1a*, *1b*, and *1c*, showing the numbering scheme used for all of the inhibitors and referenced in Table 2.

[7] The native position ($\chi_1 = 60°$) has also been called the "in" conformation, and the alternative position ($\chi_1 = -60°$) has been called the "out" conformation (Nair & Christianson, 1991).

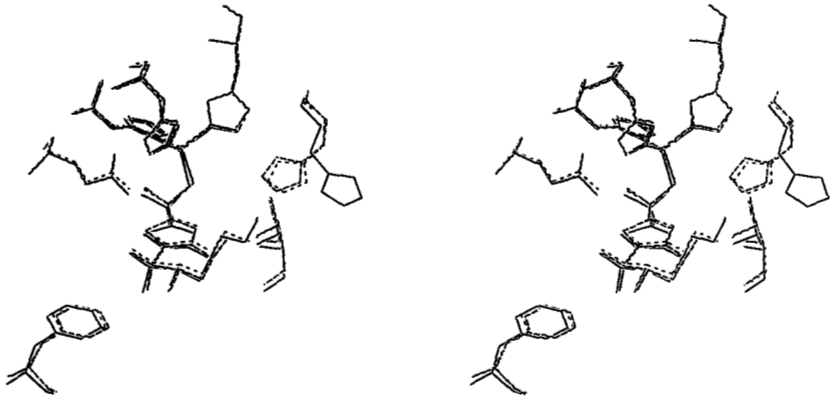

Fig. 2. Inhibitors *1a* (long dash), *1b* (short dash), *1c* (solid lines) are shown as bound to the active site. To the top are the 3 histidines binding the zinc ion (94, 96, and 119). Moving clockwise, next His-64, Thr-200, Phe-131, and Gln-92 are shown. This orientation of the active site will serve as the reference for other plots and figures.

but the increase from inhibitor *1b* to *1c* is about the same as the increase from inhibitor *1a* to *1b* and does not seem to explain the nonuniform change in the binding constants. The water adjacent to His-64 appears to make 2 hydrogen bonds, one to His-64 and a second to another ordered water. Therefore, it appears that 2 hydrogen bonds need to be broken to remove the water. When His-64 moves into the alternate position it remakes one of these hydrogen bonds to the second ordered water (2.76 Å).

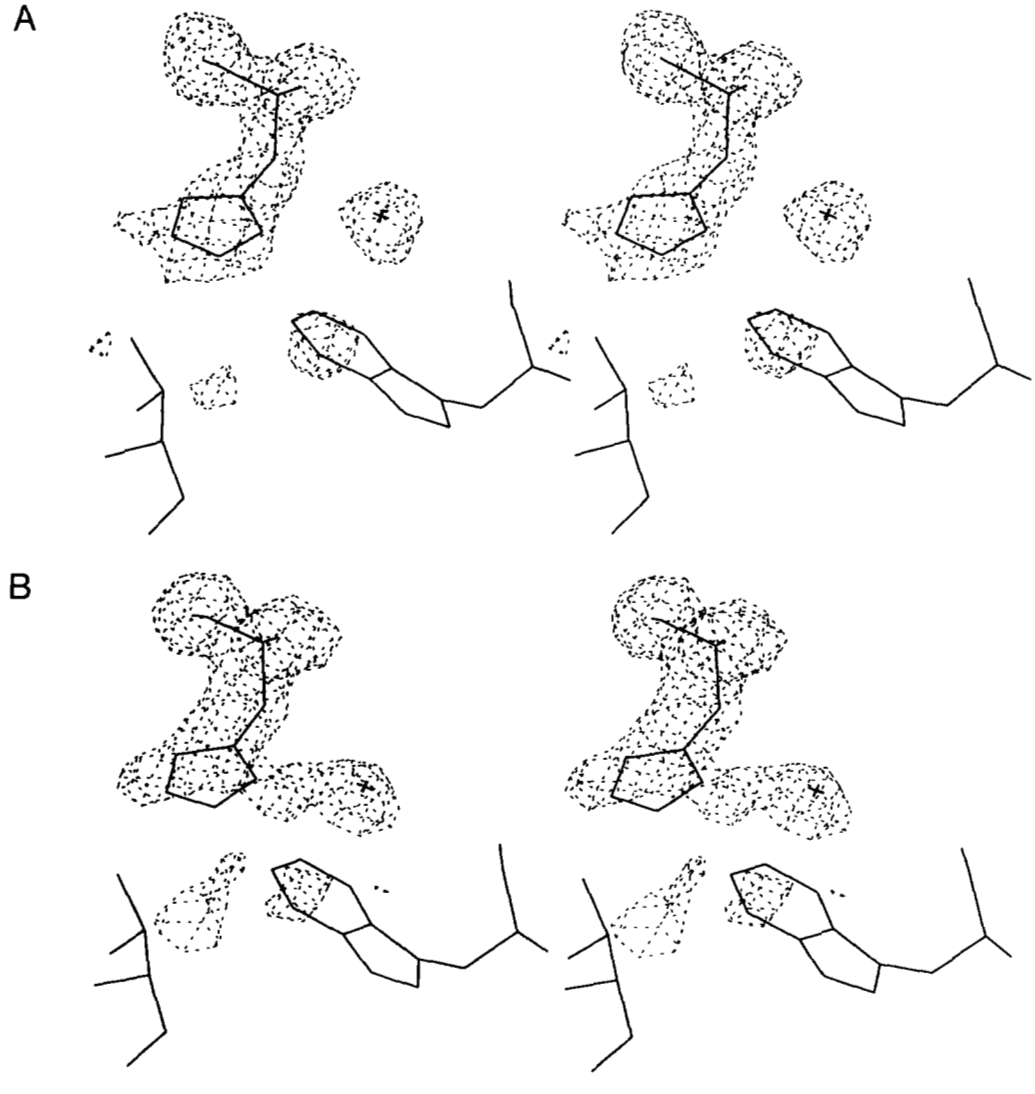

Fig. 3. Stereo views of the $|F_o| - |F_c|$ omit maps contoured at 2σ for the density around His-64 in the *1a* (**A**), *1b* (**B**), *1c* (**C**), and native (**D**) structures. (*Continues on facing page.*)

The water that is released can also make new hydrogen bonds to bulk water, gaining back the other lost hydrogen bond plus several others.

A qualitative analysis relating the structural differences in the enzyme/inhibitor complexes with the binding constants was undertaken. The change from structure *1a* to *1b* was simply to replace a proton on the primary amine with a methyl group. This change will increase the conformational flexibility and the entropic cost of fixing the position of the side chain upon binding. However, at the same time, *1b* has slightly more surface area than *1a*, and therefore more free energy will be gained when *1b* is removed from solvent upon complexation with the enzyme. Since the binding constants for *1a* and *1b* are virtually identical, the net result appears to be that the contributions from the loss of conformational entropy of the methyl group is almost exactly balanced by the desolvation of the methyl group.

On going from *1b* to *1c*, the addition of the second carbon atom allows for greater conformational flexibility and therefore a corresponding increase in entropic cost when the ethyl group is fixed in position on binding. At the same time, the new methylene provides additional surface area in *1c* with a corresponding gain in desolvation energy upon complexation. These factors, if similar in magnitude, could again almost balance, as for *1a* versus *1b*. However, the HCAII/*1c* complex has additional contributing factors: the new position of the His-64 side chain and the displacement of an ordered water molecule. For a histidine in isolation, the energy penalty required to move the side chain from the native conformation to the alternative conformation is calculated, using a relative of the MM2 force field (Weber et al., 1991), to be approximately 0.4 kcal/mol. The length of the 4-aminoethyl is sufficient to move the His-64 side chain and displace the ordered water to free solution; this entropic gain from the water molecule displacement will provide increased binding energy. The degree of increase that can be obtained is a function of how tightly bound and well ordered the water molecule is within the active site. Given that the entropy of liquid water is 16 e.u. (4.8 kcal/mol) at 25 °C, this value must represent the theoretical maximum entropy gain for the displacement of a firmly immobilized, protein-bound solvent molecule into bulk solvent. The thermal *B*-factor of this water molecule in the native enzyme is 13 $Å^2$, which is indicative of a fairly well bound water molecule. From the Boltzmann equation it can be estimated that at 300 K, a ratio of 5 in the binding constants results from a difference of about 1 kcal/mol in the 2 binding free energies of *1b* and *1c*. Therefore, we suggest that the displacement of the water adjacent to His-64 may result in a change of

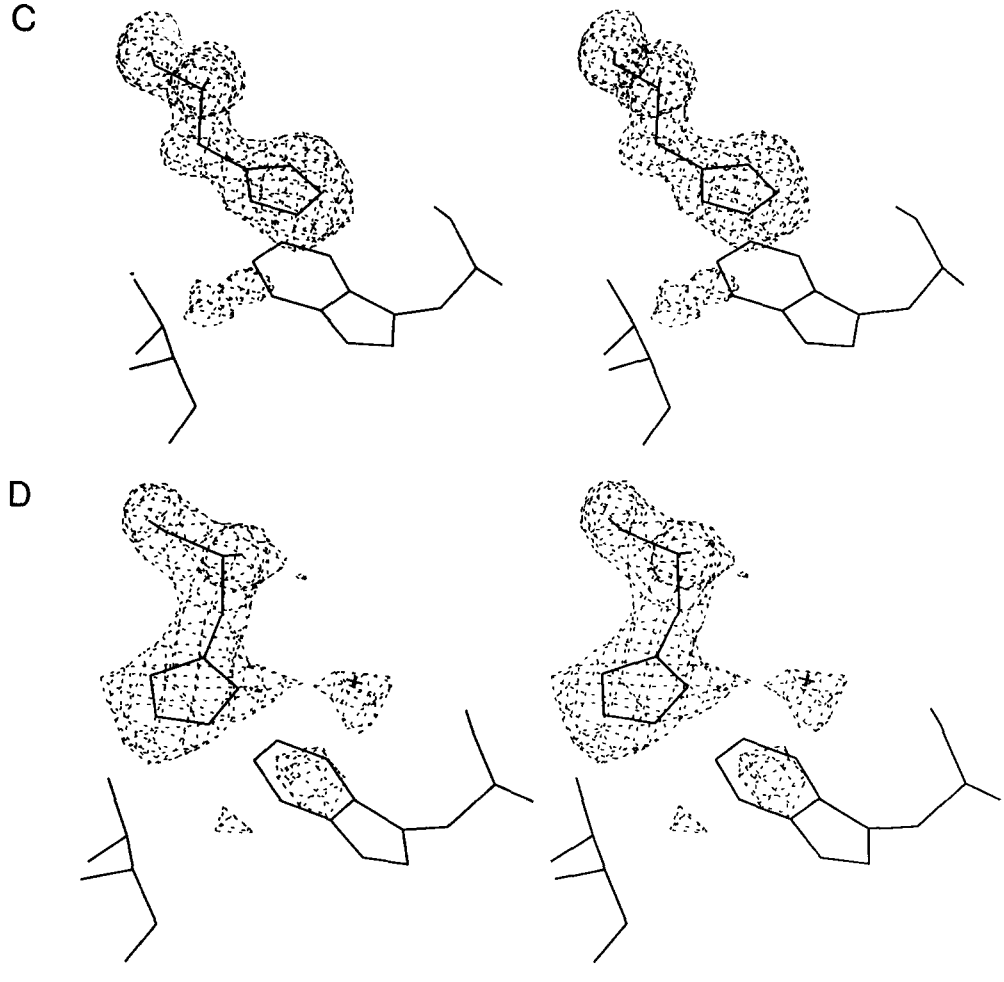

Fig. 3. *Continued.*

Table 2. *Table of distances between the atoms of the 4-amino side chains in each inhibitor (1a, 1b, and 1c) and all atoms in the protein within 4.50 Å*[a]

	N14			C18			C19		
1a	H64	NE2	3.92						
	H64	CE1	4.08						
	T200	OG1	3.06						
	T200	CB	4.34						
	P201	O	4.00						
	O328	O	4.16						
	O401	O	2.97						
	O422	O	3.40						
1b	H64	NE2	3.69	H64	NE2	3.36			
	H64	CE1	4.28	H64	CD2	4.39			
	T200	OG1	3.31	H64	CE1	3.50			
	T200	CB	4.48	W5	CZ2	4.27			
	P201	O	4.50	T200	OG1	3.48			
	O328	O	4.00	T200	CB	4.46			
	O401	O	3.50	P201	O	3.78			
	O422	O	3.60	O401	O	4.49			
				O422	O	3.85			
1c	T200	OG1	3.24	W5	CZ2	4.39	H64	CD2	3.96
	T200	CB	4.47	T200	OG1	3.39	H64	CG	4.39
	P201	O	4.48	T200	CB	4.44	H64	CB	4.30
	O325	O	4.43	P201	O	3.88	W5	CH2	4.13
	O393	O	4.28	O300	O	3.65	W5	CZ2	4.05
	O406	O	2.92	O406	O	3.85	N62	ND2	4.05
	O462	O	3.97	O462	O	4.17	T200	OG1	4.01
							O300	O	4.43
							O325	O	4.22
							O393	O	3.81
							O406	O	3.86
							O462	O	4.34

[a] See Figure 1 for atom labels. All values in Ångstroms.

free energy of about 1.4 kcal/mol to be able to overcome the energy penalty of placing the His-64 side chain into a higher energy conformation and to result in a higher affinity toward *1c*. Detailed K_i measurements made over a range of temperatures might reveal more about the energy budget for this process.

Given that the displacement of a specific, enzyme-bound water molecule into bulk solvent may account for activity differences between HCAII inhibitors *1c* and *1a* (or *1b*), it is interesting to note that analogous solvent displacement events in other systems may account for free energy differences in enzyme–inhibitor association. For example, the statine hydroxyl group of pepstatin displaces a water molecule and hydrogen bonds to the catalytic residues Asp-32 and Asp-220 in the active site of the *Rhizopus chinensis* aspartic protease (Bott et al., 1982), and a similar binding mode is observed in the complex between a statine peptide and penicillopepsin (James et al., 1982). Based on the estimations of Jencks (1976), Rich (1985) pointed out that the displacement of an enzyme-bound water molecule into bulk solvent results in 3–5 kcal/mol of energy favorable to inhibitor binding. This estimation is consistent with free energy differences measured for the enhanced binding of statine-containing peptides relative to their dideoxy analogs, which presumably cannot displace the water molecule hydrogen bonded to the active site aspartate residues.

One other difference between these 3 structures was that the procedure used to solve the *1c* structure called for the removal of the mercury ion, used to prevent the growth of twinned crystals, prior to data collection. The mercury ion was not removed from the crystals of the *1b* and *1c* complexes. To investigate the effects of solving the structures with the mercury ion present, a visual inspection was made of the region of the protein between the mercury and His-64 for both structures *1a* and *1b*. The mercury is 17.9 Å from the closest atom on the histidine in both cases. A comparison of the positions of the side chains in the region between the mercury and the histidine in structures *1a* and *1b* versus *1c* indicates that the mercury has not had a long-range effect. The only region that appears to have been disturbed involves residues Val-134 to Gln-136, which are in van der Waals contact with the mercury. The Cα of Gln-135 has been displaced by 0.87 Å from its position in the *1c* structure.

Conclusions

The crystal structures of HCAII containing inhibitors *1a* and *1b* were solved to a resolution of 2.1 Å and compared to those of the complex HCAII/*1c* solved to a resolution of 1.6 Å and the native structure. In the *1a* and *1b* inhibited forms of HCAII, the His-64 side chain is observed to be primarily in the native position. In the *1c* inhibited form of HCAII, the His-64 side chain is forced to the alternate position by the size of the 4-aminoethyl group with displacement of the adjacent water molecule. The measured K_i's for these inhibitors show a nonlinear pattern; the K_i values for *1a* and *1b* are nearly identical, whereas *1c* binds 4–5-fold more tightly. Although it is difficult to precisely break down the 1-kcal/mol preference in binding of *1c* to HCAII into its component parts, it appears that most of the difference may be explained by the release of 1 ordered water molecule. This conclusion is based on the identical alignment and interaction of the homologous series *1a*–*1c* within the active site cavity. These similarities reduce the variables of solvation, conformational energies, entropy, van der Waals forces, angle bending, and bond stretching and allow changes in binding constants to be attributed to the energetics involved in the displacement of an ordered water.

Materials and methods

HCAII/inhibitor complexes *1a* and *1b* were crystallized using the following procedure. Human carbonic anhydrase II was isolated from human erythrocytes by lysis of the cells followed by affinity chromatography (Osborne & Tashian, 1975) to give pure enzyme as judged by SDS gel electrophoresis. This material was concentrated in the isolation buffer using an Amicon Centriprep-10 concentrator; 100 mL of initial enzyme solution containing 25 mg of protein (as determined at 280 nm, $e = 0.5348$ mg·cm/mL) was concentrated to 19 mg/mL of protein. The buffer was then exchanged 3 times by dilution of the sample in a 1:10 ratio with crystallization buffer (150 mM NaCl, 50 mM Tris, 3 mM NaN_3, pH 8.0, at room temperature) followed by concentration to the original volume. All work was done at 4 °C. Crystals of the inhibited enzyme were grown by co-crystallization using the sitting drop method in the crystallization buffer described above. The concentration of the enzyme in the crystal-

lization solution was 8 mg/mL. Two solutions of each of the inhibitors were prepared using both methanol and water as solvent. The concentrations were made up so that the inhibitor solution was added in the ratio of 1:20 (v/v) to produce a final inhibitor:enzyme concentration of 2:1 in the crystallization solution. All crystallizations were done at 4 °C with 2 equivalents of $CH_3HgCO_2CH_3$ present in the buffer and enzyme solutions to reduce the incidence of twinning. Crystals of typical dimensions 0.2 × 0.3 × 0.5 mm generally formed in the wells with 62–67% ammonium sulfate in about 1 week. The mercury ion was not removed prior to mounting and data collection for inhibitors *1a* and *1b*. The crystallization attempts with the inhibitor in methanol were generally as successful as those in which water was used as the solvent.

HCAII/inhibitor complex *1c* was crystallized by methods similar to those described above, with several modifications. HCAII at 20 mg protein/mL was incubated with a sufficient quantity of inhibitor *1c* to yield a final inhibitor:enzyme ratio of 1.2:1.0. To this solution, CH_3HgCl dissolved in methanol was added to a final concentration of about 1 mM and less than 5% methanol. The protein solution was centrifuged at 15,000 × *g* for about 15 min to pellet any precipitate or debris. Micro dialysis buttons (20 μL capacity; Cambridge Repetition Engineers Ltd.) were filled with enzyme/inhibitor complex solution and sealed with a 3,500-molecular weight-cutoff dialysis membrane. Each button was placed in a scintillation vial containing 5 mL of 52–58% saturated ammonium sulfate buffered with 50 mM Tris/Tris·HCl, pH 8.5, 3 mM NaN_3 and allowed to stand undisturbed in a cold room (4–6 °C) for at least 2 weeks. Prior to collecting any diffraction data, the CH_3HgCl was removed by adding 50 μL of 1 M Cys (buffered with Tris base to pH 8.5) to each vial. Treated vials were allowed to stand no more than 3–4 days in the cold room before washing out the cysteine with fresh buffered 58% saturated ammonium sulfate.

Crystals were mounted in sealed 0.5-mm glass capillaries with a small portion of mother liquor. Data were collected using a Siemens X-100A multiwire area detector that was mounted on a 3-axis camera and equipped with Charles Supper double X-ray focusing mirrors. CuK_α radiation was supplied by a Rigaku RU-200 rotating anode generator operating at 45 kV/65 mA. All data were collected at room temperature by the oscillation method. The crystal-to-detector distance was fixed at 10 cm, and the detector swing angle was set to −25° for *1a* and *1b* and −35° for *1c*. For the *1a* and *1b* complexes, data frames of 0.0833° oscillations about omega were collected with exposure times of 60 s per frame, whereas for the *1c* complex 0.25° oscillations were used with 300-s exposures. Each data set collected spanned the range from 73° to 110° in omega. In these experiments, 4 data sets were collected to 2.1 Å using 1 crystal for inhibitor *1a*, 6 data sets were collected to 2.1 Å using 3 crystals for inhibitor *1b*, and 3 data sets were collected to 1.6 Å using 1 crystal for inhibitor *1c*. Crystals of all 3 inhibitors were isomorphous with those obtained from the native enzyme.

Raw data were analyzed and merged using the XENGEN suite of programs (Howard, 1990) to give the final indexed reflections. The relevant data reduction statistics are presented in Table 3. Wilson plots (Wilson, 1942) revealed that the data for inhibitors *1a* and *1b* were usable to 2.1 Å, while the *1c* complex was usable to 1.6 Å. Model building was started using the refined native structure (Eriksson et al., 1988) as taken from the Protein Data Bank (Bernstein et al., 1977). To begin the refinement, the waters in the native structure were removed and the structure refined for 10 cycles with PROLSQ (Hendrickson, 1985), using the data from inhibitor *1a*. The resulting coordinates were used to generate $2|F_o| - |F_c|$ and $|F_o| - |F_c|$ maps with the PROTEIN program (Steigemann, 1974). Contouring the $|F_o| - |F_c|$ map at 2σ revealed the location of the mercury ion bound to Cys-206. A model of a new residue type, Cys-Hg-CH_3, was constructed using data collected from the Cambridge Crystallographic Database (Allen et al., 1983). The search of the database revealed 30 structures containing the substructure "C-S-Hg-C". The distances, angles, and dihedrals derived from these structures were used to construct an idealized version of the new residue. The new residue was used in place of Cys-206 and was also built into the PROLSQ dictionary. Refinement was continued for an additional 30 cycles with PROLSQ. At this point, an $|F_o| - |F_c|$ map clearly revealed the location of the inhibitor in the active site. A model of *1a* was built and docked into the map using CHAIN (Sack, 1988) on a Silicon Graphics workstation. Once the inhibitor model was positioned by hand, it was refined with PROLSQ until the *R*-factor was less than 0.20, at which point the original waters were included in the structure. Waters that were within van der Waals contact of the inhibitor were removed. This model was then refined for 30 cycles with PROLSQ.

$|F_o| - |F_c|$ and $2|F_o| - |F_c|$ maps were used to review the structure and reposition side chains of some surface lysine and arginine residues and a few waters, and refinement was continued using the X-PLOR program (Brunger et al., 1990). At first, the temperature factors were held at 15.0 $Å^2$ and just the atomic positions were refined. This was followed by refinement of in-

Table 3. *Data collection statistics for inhibitors 1a, 1b, and 1c bound to carbonic anhydrase II*

	1a	*1b*	*1c*
No. of crystals	1	3	1
Space group	$P2_1$	$P2_1$	$P2_1$
a	42.72 Å	42.83 Å	42.87 Å
b	41.93 Å	42.04 Å	42.13 Å
c	72.69 Å	72.62 Å	72.92 Å
Beta	104.77°	104.78°	104.55°
No. of measured reflections[a]	32,456	32,557	57,372
No. of unique reflections	20,135	21,019	31,790
Resolution	2.1 Å	2.1 Å	1.6 Å
R_{merge}[b]	0.091	0.078	0.030
No. reflections in final refinement (6.0-Å)	12,995	13,229	28,952
No. of waters in final refinement	159	159	194
R-factor[c]	0.175	0.172	0.174
Overall temperature factor	13.0 $Å^2$	13.4 $Å^2$	14.0 $Å^2$
RMS deviation from ideal bond length	0.012 Å	0.011 Å	0.012 Å
RMS deviation from ideal bond angle	2.90°	2.80°	2.65°
RMS deviation from ideal planarity and ideal chirality	1.18°	1.15°	1.10°

[a] As reported by XENGEN, no cutoff used.
[b] $R_{merge} = \sum|I_j(h) - \langle I(h)\rangle|/\sum I_j(h)$.
[c] As reported by X-PLOR.

dividual isotropic temperature factors, holding the coordinate positions fixed. The final coordinates were produced by a last step of coordinate refinement using the individual temperature factors derived in the second step. The results are summarized in Table 3. To produce the omit maps of His-64 and adjacent water, the residue and the water were removed and the structure refined with X-PLOR. X-PLOR was then used to produce the $|F_o| - |F_c|$ maps of the region around His-64.

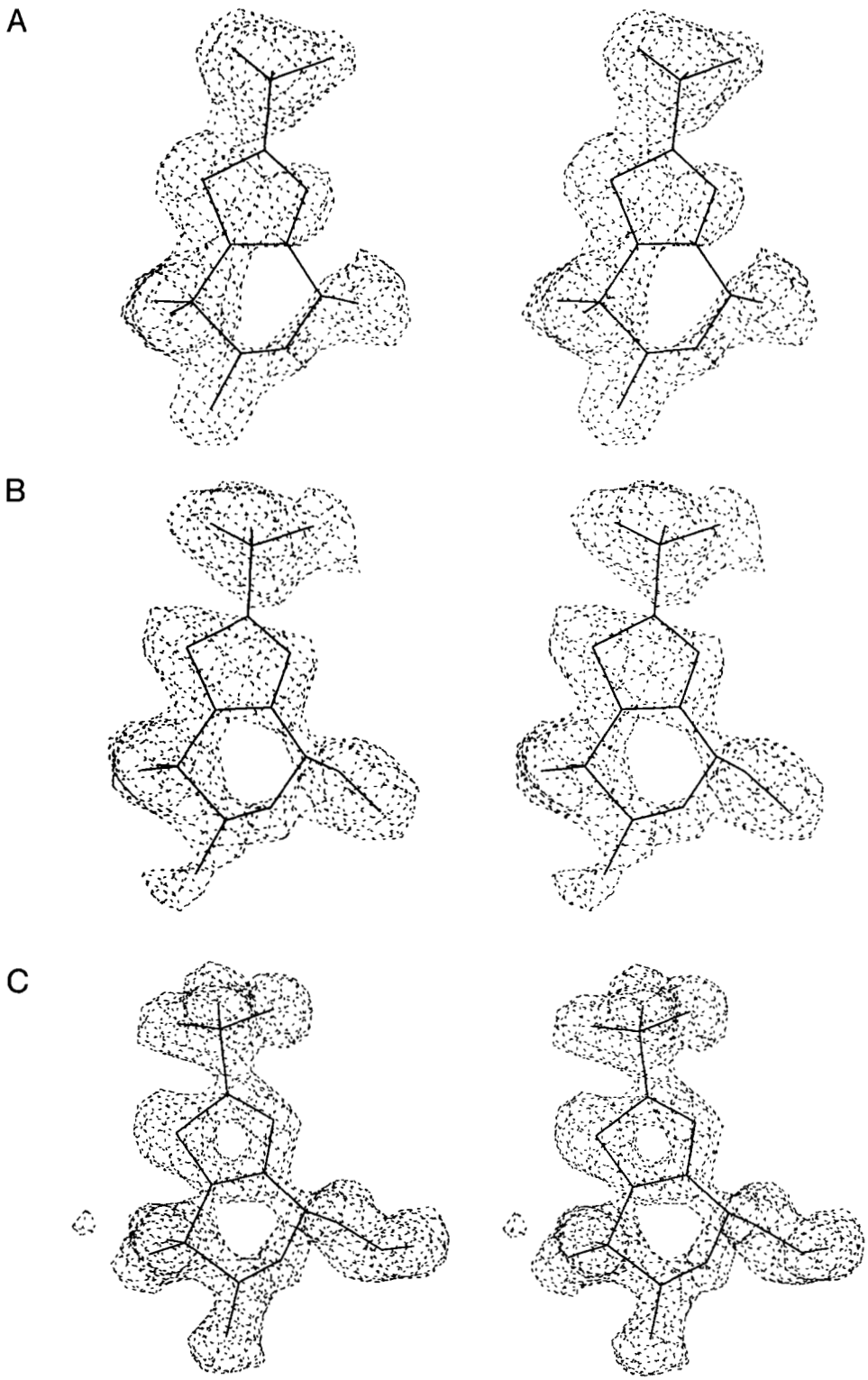

Fig. 4. Stereo views of the $|F_o| - |F_c|$ omit maps contoured at 2σ for inhibitors *1a* (**A**), *1b* (**B**), and *1c* (**C**).

Model building for inhibitor *1b* was begun using the coordinates for structure *1a* taken just after the last PROLSQ refinement was completed on *1a*. The coordinates for inhibitor *1a* and the waters were removed, and the model was refined with PROLSQ for 10 cycles using the data from inhibitor *1b*. $|F_o| - |F_c|$ maps were used to locate the inhibitor in the active site. From this point, the procedure followed was essentially the same as for structure *1a*. The structure of *1c* was solved in a manner similar to *1a* except that the mercury atom was absent and residue 206 was treated as a cysteine. Overall, the structures of the native enzyme and the 3 inhibited structures are quite similar, with RMS deviations between the Cα coordinates ranging from 0.11 to 0.29 Å. Luzzati plots (Luzzati, 1952) were made for the *1a* and *1b* structures and indicate the uncertainty in the coordinates to be 0.20 Å. $|F_o| - |F_c|$ omit maps were made for the 3 inhibitors when the refinements were done (Fig. 4). The coordinates for the 3 enzyme-inhibitor complexes described here have been submitted to the Brookhaven Protein Data Bank (Bernstein et al., 1977).

Acknowledgments

We thank J. Becker and K. Merz for helpful discussions. Grateful acknowledgment is also made to J. Sondey for the samples of human carbonic anhydrase II that were used in this work and to J. Shafer and D. Lewis for access to biochemistry laboratory space. This work was supported in part by NSF grant DIR-8821184 for the X-ray data acquisition facility at the University of Pennsylvania and a research fellowship from the Alfred P. Sloan Foundation (D.W.C.).

References

Allen FH, Kennard O, Taylor R. 1983. Systematic analysis of structural data as a research technique in organic chemistry. *Acc Chem Res 16*:146–153.

Baldwin JJ, Ponticello GS, Anderson PS, Christy ME, Murcko MA, Randall WC, Schwam H, Sugrue MF, Springer JP, Gautheron P, Grove J, Mallorga P, Viader MP, McKeever BM, Navia MA. 1989. Thienothiopyran-2-sulfonamides: Novel topically active carbonic anhydrase inhibitors for the treatment of glaucoma. *J Med Chem 32*:2510–2513.

Baldwin JJ, Smith G, Springer JP, Murcko MA. 1992. Scientists from Merck and Vertex describe role of X-ray crystallography in drug design. *Chem Design Automation News 7*:1–34.

Bernstein FC, Koetzle TF, Williams GJB, Meyer EF Jr, Brice MD, Rodgers JR, Kennard O, Shimanouchi T, Tasumi M. 1977. The Protein Data Bank: A computer-based archival file for macromolecular structures. *J Mol Biol 112*:535–542.

Bott R, Subramanian E, Davies DR. 1982. Three-dimensional structure of the complex of the *Rhizopus chinensis* carboxyl proteinase and pepstatin at 2.5-Å resolution. *Biochemistry 21*:6956–6962.

Brünger AT, Krukowski A, Erickson JW. 1990. Slow-cooling protocols for crystallographic refinement by simulated annealing. *Acta Crystallogr A 46*:585–593.

Eriksson AE, Jones TA, Liljas A. 1988. Refined structure of human carbonic anhydrase II at 2.0 Å resolution. *Proteins Struct Funct Genet 4*:274–282.

Hendrickson WA. 1985. Stereochemically restrained refinement of macromolecular structures. In: Wyckoff HW, Hirs CHW, Timasheff SN, eds. *Diffraction methods for biological macromolecules*. Orlando, Florida: Academic Press. pp 252–270.

Howard AJ. 1990. *A guide to macromolecular X-ray data reduction for the Siemens area detector system: The XENGEN system, version 2.0*. Gaithersburg, Maryland: Genex Corporation.

James MNG, Sielecki A. 1983. Structure and refinement of penicillopepsin at 1.8 Å resolution. *J Mol Biol 163*:299–361.

James MNG, Sielecki A, Salituro F, Rich DH, Hofmann T. 1982. Conformational flexibility in the active sites of aspartyl proteinases revealed by a pepstatin fragment binding to penicillopepsin. *Proc Natl Acad Sci USA 79*:6137–6141.

Jencks WP. 1976. Binding energy, specificity, and enzymic catalysis: The Circe effect. *Adv Enzymol Relat Areas Mol Biol 43*:219–410.

Krebs JF, Fierke CA, Alexander RS, Christianson DW. 1991. Conformational mobility of His-64 in the Thr-200 → Ser mutant of human carbonic anhydrase II. *Biochemistry 30*:9153–9160.

Liljas A, Kannan KK, Bergsten PC, Waara I, Fridborg K, Strandberg B, Carlbom U, Järup L, Lövgren S, Petef M. 1972. Crystal structure of human carbonic anhydrase C. *Nature New Biol 235*:131–137.

Luzzati PV. 1952. Traitement statistique des erreurs dans la détermination des structures cristallines. *Acta Crystallogr 5*:803–810.

Maren TH. 1967. Carbonic anhydrase: Chemistry, physiology, and inhibition. *Physiol Rev 47*:595–781.

Nair SK, Christianson DW. 1991. Unexpected pH-dependent conformation of His-64, the proton shuttle of carbonic anhydrase II. *J Am Chem Soc 113*:9455–9458.

Osborne WRA, Tashian RE. 1975. An improved method for the purification of carbonic anhydrase isozymes by affinity chromatography. *Anal Biochem 64*:297–303.

Pocker Y, Sarkanen S. 1978. Carbonic anhydrase: Structure, catalytic versatility, and inhibition. *Adv Enzymol Relat Areas Mol Biol 47*:149–274.

Ponticello GS, Freedman MB, Habecker CN, Lyle PA, Schwam H, Varga SL, Christy ME, Randall WC, Baldwin JJ. 1987. Thienothiopyran-2-sulfonamides: A novel class of water-soluble carbonic anhydrase inhibitors. *J Med Chem 30*:591–597.

Prugh JD, Hartman GD, Mallorga PJ, McKeever BM, Michelson SR, Murcko MA, Schwam H, Smith RL, Sondey JM, Springer JP, Sugrue MF. 1991. New isomeric classes of topically active ocular hypotensive carbonic anhydrase inhibitors: 5-Substituted thieno[2,3-*b*]thiophene-2-sulfonamides and 5-substituted thieno[3,2-*b*]thiophene-2-sulfonamides. *J Med Chem 34*:1805–1818.

Rich DH. 1985. Pepstatin-derived inhibitors of aspartic proteinases. A close look at an apparent transition-state analogue inhibitor. *J Med Chem 28*:263–273.

Sack JS. 1988. CHAIN—A crystallographic modeling program. *J Mol Graphics 6*:224–225.

Steigemann W. 1974. Die Entwicklung und Anwendung von Rechenverfahren und Rechenprogrammen zur Strukturanalyse von Proteinem am Beispiel des trypsin-trypsininhibitor Komplexes, des freien Inhibitors und der L-Asparaginase [thesis]. München: Technische Universität.

Tu C, Silverman DN, Forsman C, Jonsson BH, Lindskog S. 1989. Role of histidine 64 in the catalytic mechanism of human carbonic anhydrase II studied with a site-specific mutant. *Biochemistry 28*:7913–7918.

Weber AE, Halgren TA, Doyle JJ, Lynch RJ, Siegl PKS, Parsons WH, Greenlee WJ, Patchett AA. 1991. Design and synthesis of P_2-P_1'-linked macrocyclic human renin inhibitors. *J Med Chem 34*:2692–2701.

Wilson AJC. 1942. Determination of absolute from relative X-ray intensity data. *Nature 150*:151–152.